

Original Research

Unveiling Circular RNA-Mediated Regulatory Mechanisms in Necroptosis in Premature Ovarian Failure

Xin Jin¹, Wenjun Chen^{2,3,*}, Jiaxi Wang³, Xianli Xu³, Ting Zhang³, Lu Wang⁴, Xuehua Feng⁵¹Department of Tuina, The First Affiliated Hospital of Zhejiang Chinese Medical University, 310006 Hangzhou, Zhejiang, China²School of Nursing, Hangzhou Medical College, 311399 Hangzhou, Zhejiang, China³Department of Gynecology and Obstetrics, The First Affiliated Hospital of Zhejiang Chinese Medical University, 310006 Hangzhou, Zhejiang, China⁴Department of Lung Disease, Jining Hospital of Traditional Chinese Medicine, 272037 Jining, Shandong, China⁵Center of Reproductive Medicine, The Second Hospital Affiliated to Shandong University of Traditional Chinese Medicine, 250001 Jinan, Shandong, China*Correspondence: 20163354@zcmu.edu.cn (Wenjun Chen)

Academic Editor: Fu Wang

Submitted: 24 February 2023 Revised: 15 June 2023 Accepted: 7 July 2023 Published: 28 November 2023

Abstract

Background: Necroptosis is a programmed necrotic cell death, in which dying cells rupture and release intracellular components that trigger a proinflammatory response. The current study aimed at probing the circular RNA (circRNA)-mediated regulatory mechanisms in necroptosis in premature ovarian failure (POF). **Methods:** CircRNA sequencing analysis was conducted in ovarian tissues of control and POF rats and transcriptome microarrays were acquired from the GSE33423 dataset. Differential expression analysis of circRNAs and mRNAs was executed between the POF and control data. Both a necroptosis-based circRNA–microRNA (miRNA)–mRNA network and a protein–protein interaction (PPI) network were established. Then, the functional annotation and immunological traits were analyzed. **Results:** Totally, 1266 upregulated and 1283 downregulated circRNAs as well as 1101 upregulated and 1168 downregulated mRNAs were determined in the POF rats versus the controls. The differentially expressed mRNAs predominantly correlated with necroptosis. The circRNA–miRNA–mRNA networks of downregulated necroptosis genes (comprising rno_circRNA_004995-rno-miR-148b-5p-H2afy2, rno_circRNA_016998-rno-miR-29a-5p-Hmgb1, and rno_circRNA_017593-rno-miR-29a-5p-Hmgb1) and upregulated necroptosis genes (comprising rno_circRNA_015900-rno-miR-935-Stat1, rno_circRNA_007946-rno-miR-328a-3p-Stat5a, rno_circRNA_007947-rno-miR-328a-3p-Stat5a, rno_circRNA_005064-rno-miR-18a-5p-Stat1, rno_circRNA_005064-rno-miR-18a-5p-Stat5a, rno_circRNA_005115-rno-miR-22-3p-Stat1, rno_circRNA_009028-rno-miR-342-5p-Stat1, rno_circRNA_011240-rno-miR-1224-Stat5a, rno_circRNA_016078-rno-miR-711-Stat5a) were built. POF-specific necroptosis genes (*STAT1*, *STAT5A*, *PLA2G4A*, *HMG1L1*, *HMGB1*, *AGER*, *EGFR*, *HDAC7*, *IFNA1*, *IL10RB*, *IL27RA*, *PYGL*, *SOCS1*, *TRADD*, *CXCL10*, *DDX5*, *EZH2*, *FADS2*, *FER*, *H2AFY2*, *HIST1H2AF*, *IFI44L*, *IL27*, *IRGM*, *MX1*, *NFKB2*, *PAFAH2*, *PEMT*, *PGM2L1*, *PGR*, *PHKA2*, and *PLB1*) were selected since they displayed notable associations with most immune cells, immune checkpoints, chemokines, human leukocyte antigen (HLA) molecules, and immune receptors. **Conclusions:** Altogether, we proposed the presence of widespread regulatory mechanisms of circRNAs in necroptosis and demonstrated that altered circRNA biogenesis might contribute to POF by affecting necroptosis.

Keywords: premature ovarian failure; circRNA; necroptosis; circRNA–miRNA–mRNA network; protein–protein interaction; immunity

1. Introduction

Premature ovarian failure (POF) is a gynecological endocrine disease, which is characterized by mature follicle deficiency in women under 40 years of age, who also have reduced estrogen levels and elevated gonadotropins [1]. The global incidence of POF is 1%–3%, while there has been a gradual increase in recent years [2]. Despite the influence of POF in a small percentage of women, evidence shows that it appears to correlate to mortality [3]. Chemotherapy-induced granulosa apoptosis is a primary etiology of POF [4], which remains one of the most prevalent causes of female infertility. Currently, hormone replacement treatment represents the major therapeutic option for POF; however, it is accompanied by severe side effects [5]. Hence, more potent therapeutic approaches are required.

Circular RNAs (circRNAs) are a novel class of RNA molecules that possess a covalently closed circular structure and the absence of a 5'-cap and 3'-poly(A) tail, thereby offering resistance to RNA exonuclease-induced degradation [6]. CircRNAs are specifically abundant in cell types and tissues during development [7]. Despite the synthesis of circRNAs in the nucleus, they are principally localized in the cytoplasm [8]. CircRNAs are capable of binding distinct forms and numbers of microRNAs (miRNAs) as well as negatively modulate modulating miRNA activity through competitive miRNA–mRNA binding [9]. Accumulated evidence demonstrates that circRNAs display notable regulatory functions through (i) binding to the host genes at their synthesis locus and causing transcriptional pausing or termination; (ii) combining with U1 snRNP and interacting with Pol II to improve parental gene expression; (iii) act-



ing as miRNA sponges and regulating the miRNA-targeted mRNAs; (iv) interacting with proteins; (v) directly recruiting ribosomes and triggering translation, *etc.*; thus, participating in multiple physiological and pathophysiological processes in a variety of human diseases [10–12]. Nonetheless, to date, no studies have unveiled the roles of circRNAs in POF.

Necroptosis is a caspase-independent form of programmed necrotic cell death, which presents the features of an increase in cell volume, swelling of organelles, and the rupturing of the plasma membranes together with the loss of intracellular content [13]. Necroptosis is regulated by RIPK1 kinase, together with RIPK3 kinase and MLKL pseudo-kinase, and is accompanied by the release of damage-associated molecular patterns and cytokines, which triggers a 2proinflammatory response [14]. Evidence proves that necroptosis is a highly regulated and orchestrated process, which plays fundamental physiological functions in development and tissue homeostasis [15]. Dysregulation of necroptosis has been detected in diverse human diseases, including POF [16]. However, the molecular mechanisms underlying necroptosis in POF are still indistinct. Several circRNAs have been discovered to participate in necroptosis [17]. For instance, circRNA CNEACR affects necroptosis of cardiomyocytes via attenuating Foxa2 activity [17]. Nonetheless, the regulatory functions of circRNAs in necroptosis during POF remain indistinct. Herein, comprehensive research was implemented to probe for the circRNA regulatory mechanisms involved in necroptosis.

2. Materials and Methods

2.1 Experimental Animals and POF Establishment

All experimental procedures were approved by the Animal Ethical and Welfare Committee of Zhejiang Chinese Medical University (IACUC-20210503-05). A total of 6 female Sprague Dawley (SD) rats (3-week-old, and 50 ± 5 g in weight) had free access to adequate food and water and were adaptively fed for 1 week. All rats were randomly separated into POF and control groups. To establish POF models, rats were administered intraperitoneally with 80 mg/kg 4-vinylcyclohexene diepoxide (VCD) solution, which had been dissolved in 2.5 mL/kg/day sesame oil, for 15 consecutive days. Control rats did not receive any treatment. The ovaries were collected under anesthesia 45 days after the initial treatment, and stored at -80°C .

2.2 CircRNA Sequencing

RNA-seq analysis of the ovaries was conducted by Aksomics Inc. (Shanghai, China). Briefly, total RNA was extracted using TRIzol reagent (Invitrogen, catalog number 15596026, Thermo Fisher, New York, NY, USA), and twice treated with DNase I (Ambion, catalog number EN0521, Thermo Fisher, New York, NY, USA) for 30 min at 37°C . Next, 3 μg extracted RNA was subjected

to RiboMinus Eukaryote Kit (catalog number A15020, life technologies, New York, NY, USA) to remove any ribosomal RNA, and subsequently treated with RNase R (catalog number RNR07250, epicentre, Epicentre Biotechnologies, Madison, WI, USA). Purified RNA was treated with RNase R and purified with Trizol. Next, a RNA sequencing library was constructed, and raw sequencing data were achieved on the Illumina NovaSeq 6000. Quantile normalization and data preprocessing were performed using the limma computational approach [18]. Our circRNA RNA-seq data were uploaded into the Gene Expression Omnibus repository with the accession number GSE221728.

2.3 Dataset Acquisition

Transcriptome microarrays from POF granulosa cells ($n = 3$) and controls ($n = 3$) were acquired from the GSE33423 dataset in the Gene Expression Omnibus repository [19]. This dataset was based on the Affymetrix platform.

2.4 Differential Expression Analysis

Expression levels of circRNAs and mRNAs were compared between POF and control groups using limma [18]. For differentially expressed circRNAs, the criteria were set as $|\text{fold change (FC)}| > 1.5$ and $p\text{-value} < 0.05$. Furthermore, mRNAs with differential expressions were screened based upon $|\text{FC}| > 1.2$ and $p\text{-value} < 0.05$.

2.5 Prediction of circRNA–miRNA and miRNA–mRNA Interactions

The CircAtlas 2.0 database, which is an integrated resource of 1,007,087 circRNAs from 1070 RNA-seq profiles acquired from 19 normal tissue specimens among 6 vertebrate species [20], was adopted to infer the interactions between circRNAs and miRNAs. Through utilizing three online databases comprising miRanda [21], miRDB [22], and miTarBase [23], miRNAs that targeted down- or upregulated mRNAs were estimated and intersected through any two databases. After integrating the circRNA–miRNA and miRNA–miRNA relationships, Cytoscape software (version 3.7.2, The Cytoscape Consortium, San Diego, CA, USA) was used to establish the competitive endogenous RNA (ceRNA) networks [24].

2.6 Protein–Protein Interaction

To evaluate the interactions between proteins derived from mRNAs with differential expression, they were imported into the STRING online tool using the criteria of required confidence (combined score) > 0.2 [25]. Protein–protein interaction (PPI) network and subnetwork were constructed using Cytoscape software [24].

2.7 Functional Annotation Analysis

Gene Ontology [26] and Kyoto Encyclopedia of Genes and Genomes (KEGG) [27] analyses were used to

analyze the functional annotations of mRNAs with differential expression or those from the ceRNA network. A *p*-value was computed by Fisher's exact test. KEGG pathways were integrated and visualized using the Pathview web tool [28].

2.8 Gene Set Enrichment Analysis

To gain insights into the biological processes as well as to predict the signaling pathways underlying POF-specific necroptosis genes, gene set enrichment analysis (GSEA) was performed to determine the differences in predefined gene sets between low and high expression groups using GSEA software (GSEA4.3.2, Broad Institute, Massachusetts, USA), which was acquired from the Broad Institute website, to divide the median expression value of each gene [29]. Terms with a false discovery rate (FDR) < 0.05 were regarded as being statistically different.

2.9 Analysis of Immunological Traits

The abundance levels of 28 immune cell types were estimated by conducting single-cell GSEA (ssGSEA) [30]. Marker genes of immune signatures were acquired from previously reported literature [31,32]. Then, the transcriptional levels of immune checkpoints, chemokines, HLA molecules, and immune receptors were measured.

2.10 Statistical Analysis

Student's *t* test was performed to compare the two groups. Pearson's test was executed for correlation analysis. All statistical analyses were implemented utilizing appropriate R packages, and a *p*-value < 0.05 was regarded as being statistically different.

3. Results

3.1 Characterization of circRNAs with Differential Expression in POF

To identify the circRNAs linked to POF, the current study implemented circRNA sequencing analysis of POF (n = 3) and control (n = 3) rats. CircRNAs with differential expression in POF versus controls were screened based upon the criteria of |FC| > 1.5 and *p*-value < 0.05. Consequently, 1266 circRNAs displayed notable upregulation in POF, with 1283 displaying downregulation (Fig. 1A–C). Especially, according to |FC|, we listed the top twenty up- and downregulated circRNAs in POF versus the controls (Fig. 1D; Table 1).

3.2 Characterization of mRNAs with Differential Expression in POF

Using the GSE33423 dataset, we acquired transcriptome microarrays of granulosa cells from POF rats (n = 3) and controls (n = 3). In accordance with the criteria of |FC| > 1.2 and *p*-value < 0.05, 1101 upregulated and 1168 downregulated mRNAs were determined in POF versus the controls (Fig. 2A–C). Fig. 2D and Table 2 exhibit the top twenty up- and downregulated mRNAs in POF.

Table 1. The top twenty up- or down-regulated circRNAs in Premature Ovarian Failure (POF).

CircRNA	FC	<i>p</i> -value	POF	Control
rno_circRNA_000533	8.817872	0.011922	11.59819	8.45776
rno_circRNA_009919	7.982057	0.044604	10.1221	7.125338
rno_circRNA_006470	7.455418	0.011668	11.74922	8.850927
rno_circRNA_013584	4.813815	0.016983	8.657626	6.390445
rno_circRNA_006302	4.755354	0.006808	9.295672	7.046120
rno_circRNA_010219	4.486212	0.017652	9.214423	7.048926
rno_circRNA_012252	4.450755	0.002685	10.29526	8.141205
rno_circRNA_016249	4.428738	0.017816	10.35168	8.204789
rno_circRNA_000793	4.382331	0.029822	13.02908	10.89738
rno_circRNA_011190	4.009956	0.003978	14.4195	12.41592
rno_circRNA_014301	4.009926	0.005692	12.50601	10.50243
rno_circRNA_000744	3.89185	0.036171	7.79587	5.835414
rno_circRNA_015435	3.838654	0.010209	8.26612	6.325519
rno_circRNA_010731	3.705022	0.006016	10.34953	8.460048
rno_circRNA_004711	3.659872	0.043366	13.83036	11.95857
rno_circRNA_003801	3.649891	0.004511	9.219965	7.352112
rno_circRNA_014213	3.621472	0.009671	8.726146	6.86957
rno_circRNA_014697	3.518985	0.009275	8.307949	6.492789
rno_circRNA_016250	3.501406	0.016538	9.076473	7.268539
rno_circRNA_013867	3.305436	0.042433	9.29857	7.573730
rno_circRNA_010908	-4.061626	0.04952	8.885084	10.90714
rno_circRNA_010915	-3.991287	0.041435	9.066669	11.06352
rno_circRNA_016089	-3.704793	0.01211	10.07340	11.96279
rno_circRNA_010899	-3.514956	0.030103	8.954184	10.76769
rno_circRNA_008876	-3.421548	0.014662	6.818012	8.592661
rno_circRNA_016117	-3.400489	0.001901	10.14188	11.90762
rno_circRNA_010902	-3.381989	0.037659	7.887483	9.645355
rno_circRNA_014760	-3.230040	0.006623	11.50289	13.19444
rno_circRNA_002963	-3.142970	0.021231	5.789300	7.441429
rno_circRNA_010913	-3.099887	0.036277	8.177894	9.810110
rno_circRNA_005883	-3.086863	0.026067	10.17528	11.80142
rno_circRNA_005882	-3.081514	0.033885	10.29693	11.92057
rno_circRNA_005660	-3.072068	0.009121	8.645405	10.26462
rno_circRNA_010906	-2.986607	0.037284	8.198861	9.777369
rno_circRNA_003480	-2.986285	0.039800	9.770678	11.34903
rno_circRNA_012677	-2.983265	0.044019	9.761154	11.33805
rno_circRNA_017723	-2.959720	0.021731	10.71122	12.27668
rno_circRNA_014763	-2.914996	0.01344	11.61251	13.15600
rno_circRNA_007793	-2.896697	0.031253	10.58902	12.12343
rno_circRNA_016115	-2.837164	0.017310	8.701161	10.20561

FC, fold change.

3.3 Exploration of Biological Significance of mRNAs with Differential Expression in POF

Next, the current study further probed the biological significance of mRNAs with abnormal expressions. As illustrated in Fig. 3A, diverse metabolic (carboxylic acid, lipid, organic acid, cholesterol, sterol, *etc.*) and biosynthetic (steroid, isoprenoid, lipid, cholesterol, *etc.*) processes were notably enriched. In addition, mRNAs with differential expression were especially linked to intracellular

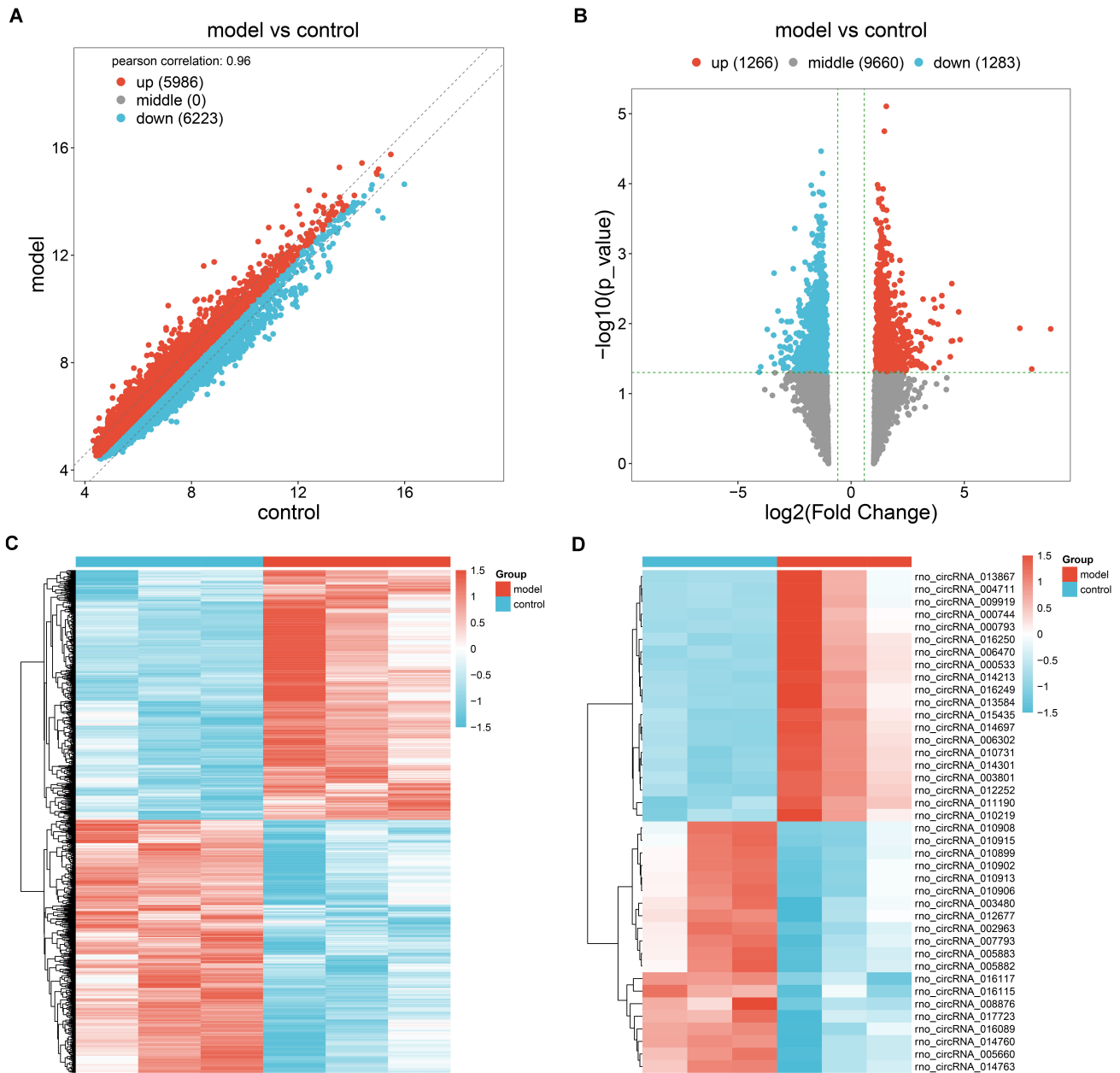


Fig. 1. Characterization of circular RNAs (circRNAs) with differential expression in premature ovarian failure (POF) rats (n = 3) versus controls (n = 3). (A,B) Scatter and volcano plots illustrate the circRNAs with differential expression in POF compared to controls based upon the criteria of $|FC| > 1.5$ together with p -value < 0.05 . Blue denotes downregulated circRNA, while red indicates upregulated circRNA. (C) Heatmap illustrates the expression levels of circRNAs with differential expression across POF and control specimens. Colors from blue to red represent downregulated to upregulated circRNA levels. (D) Heatmap depicts the top twenty up- or downregulated circRNAs in POF compared to controls.

membrane-bounded organelles (Fig. 3B) and transaminase activity (Fig. 3C). For KEGG pathway enrichment analysis, metabolic (cysteine and methionine, 2-Oxocarboxylic acid, phenylalanine, *etc.*), biosynthesis (steroid, terpenoid backbone, valine leucine and isoleucine, phenylalanine tyrosine, tryptophan, *etc.*), and necroptosis pathways were prominently correlated to mRNAs with differential expression (Fig. 3D). The accumulated evidence unveiled that necroptosis participates in gynecological endocrine diseases [33].

Nonetheless, no current studies have uncovered the function of necroptosis in POF. Notably, the necroptosis pathway was visualized, and among mRNAs with differential expression, *IFNA1*, *TRADD*, *H2AFY2*, *STAT5A*, *SPATA2*, *PYGL*, *PPID*, *PLA2G4A*, and *HMGB1* were enriched in this pathway (Fig. 3E), thereby demonstrating the potential implication of necroptosis in POF.

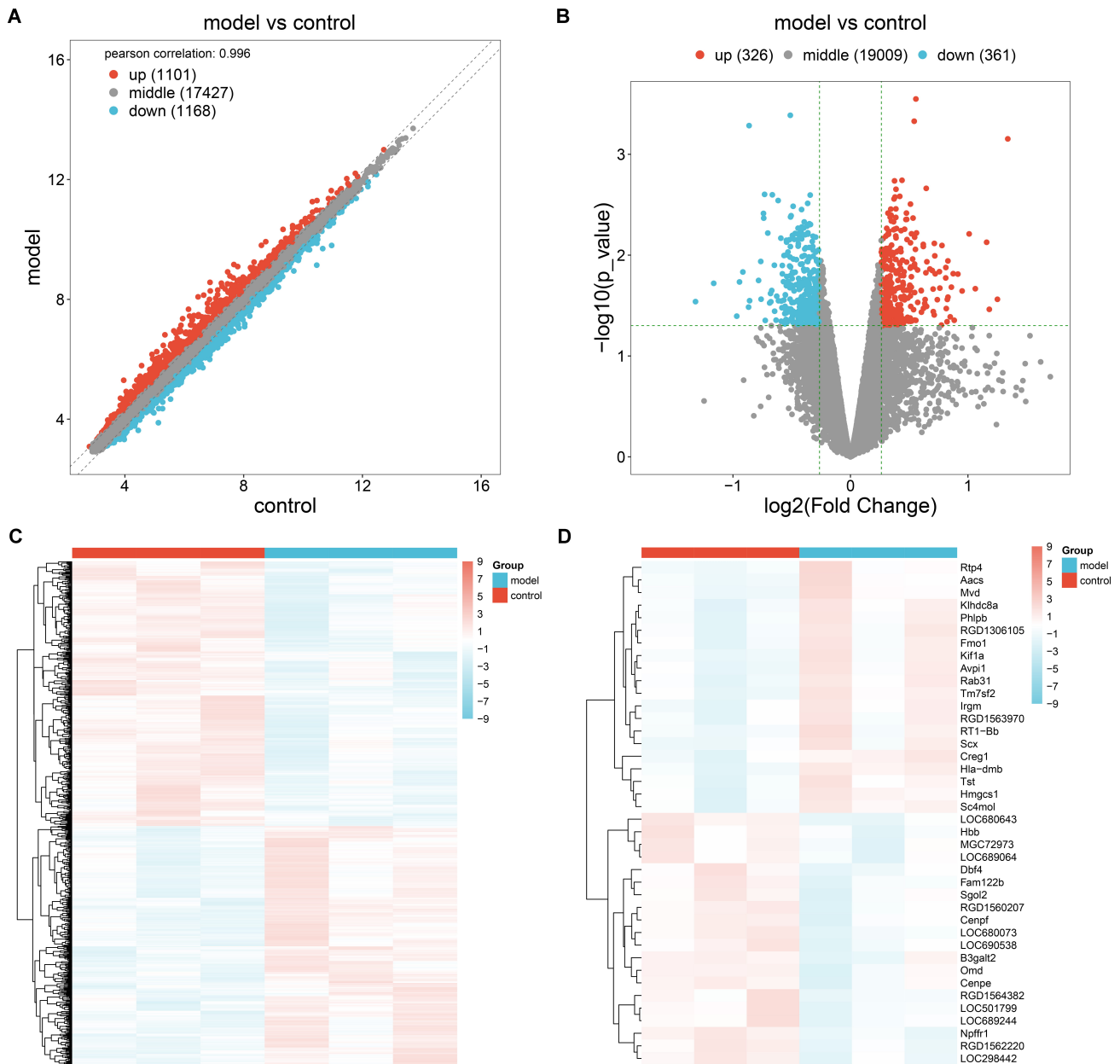


Fig. 2. Characterization of mRNAs with differential expression in POF (n = 3) versus controls (n = 3) in the GSE33423 dataset. (A,B) Scatter and volcano plots displaying the mRNAs with differential expression in POF compared to control specimens after applying the criteria of $|FC| > 1.2$ together with $p\text{-value} < 0.05$. Blue represents downregulated mRNA and red indicates upregulated mRNA. (C) Heatmap exhibits the expression levels of mRNAs with differential expression across POF and controls. Colors from blue to red denote downregulated to upregulated mRNA levels. (D) Heatmap illustrates the top twenty up- or downregulated mRNAs in POF versus control specimens.

3.4 Establishing Necroptosis-Based circRNA-miRNA-mRNA Networks in POF

Next, the circRNA-targeted miRNAs with differential expressions were inferred from the CircAtlas 2.0 database. Totally, there were 82 circRNA-miRNA relationships in the POF dataset (**Supplementary Table 1**). By integrating any two databases (miRDB, miRanda, and miTarBase), a total of 271 miRNAs were estimated that potentially targeted the downregulated mRNAs (Fig. 4A) and 3 miRNAs

that potentially targeted the upregulated mRNAs (Fig. 4B). Thereafter, circRNA-miRNA-mRNA regulatory networks were comprised (**Supplementary Table 2**). Fig. 4C depicts the circRNA-miRNA-mRNA network of downregulated necroptosis genes, comprising rno_circRNA_004995-rno-miR-148b-5p-H2afy2, rno_circRNA_016998-rno-miR-29a-5p-Hmgb1, and rno_circRNA_017593-rno-miR-29a-5p-Hmgb1. In addition, Fig. 4D illustrates the circRNA-miRNA-mRNA network of upregulated necrop-

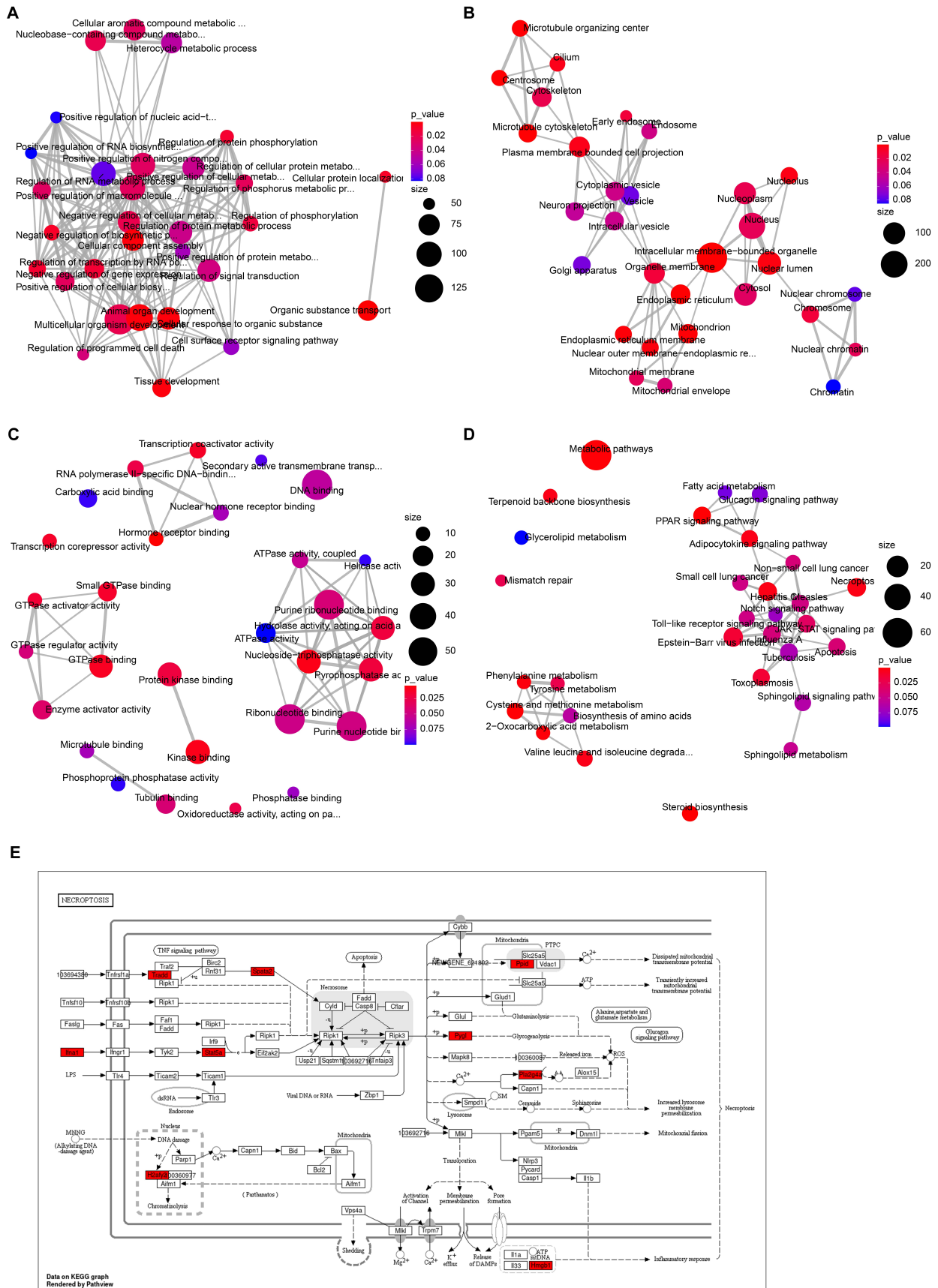


Fig. 3. Exploration of the biological significance of differentially expressed mRNAs in POF. (A) Biological process, (B) cellular component, (C) molecular function, and (D) Kyoto Encyclopedia of Genes and Genomes (KEGG) pathway terms for mRNAs with differential expression. (E) Visualization of necroptosis pathway enriched by mRNAs with differential expression.

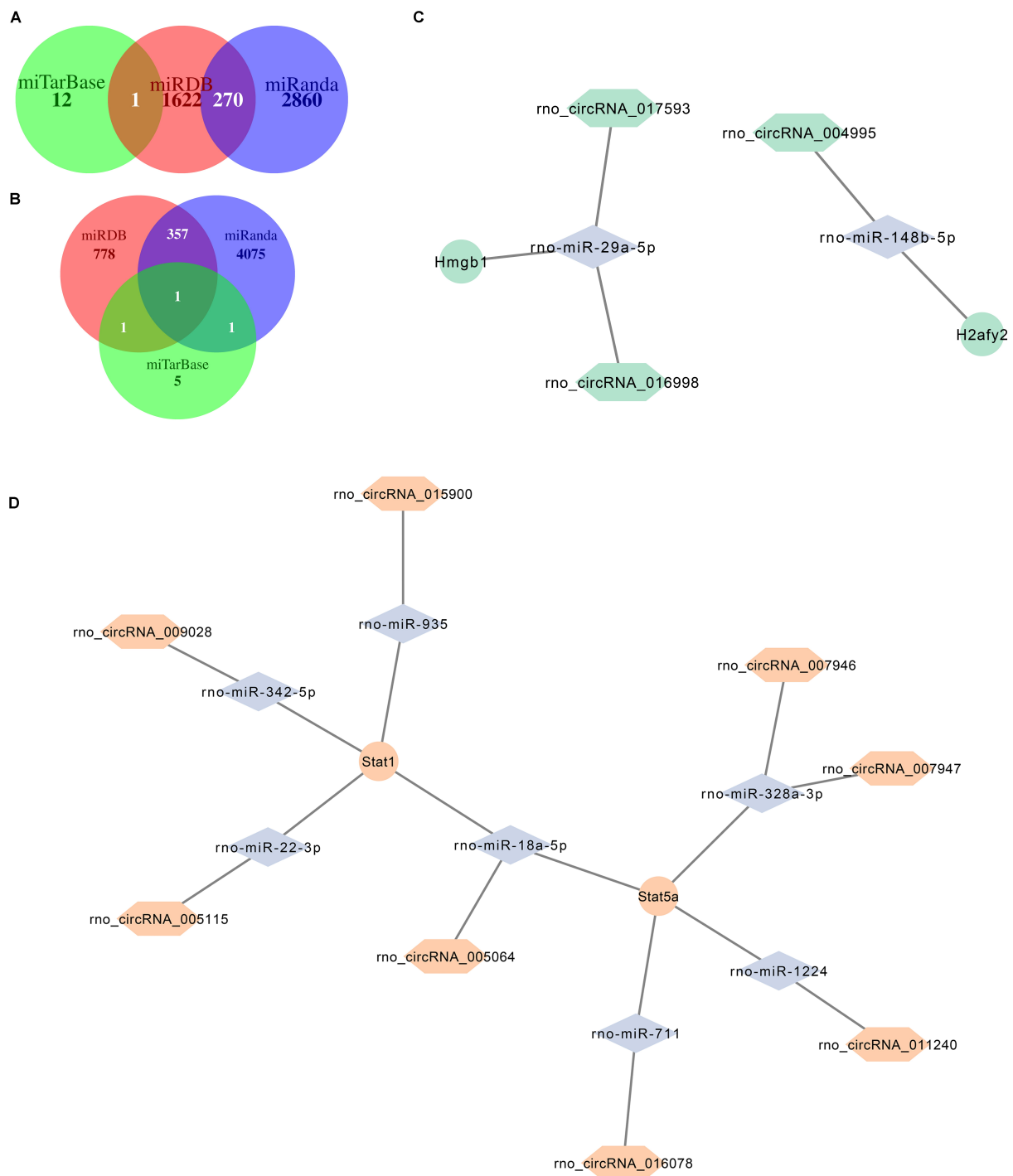


Fig. 4. Establishment of necroptosis-based circRNA–miRNA–mRNA networks in POF. (A) Venn diagram depicting the microRNAs (miRNAs) of the downregulated mRNAs by integrating any two databases from miRDB, miRanda, and miTarBase. (B) Venn diagram exhibiting the miRNAs of the upregulated mRNAs by integrating any two databases from miRDB, miRanda, and miTarBase. (C) The circRNA–miRNA–mRNA network of downregulated necroptosis genes. Hexagon: circRNA; diamond: miRNA; circle: mRNA. (D) The circRNA–miRNA–mRNA network of upregulated necroptosis genes.

osis genes, which is composed of rno_circRNA_015900-rno-miR-935-Stat1, rno_circRNA_007946-rno-miR-328a-3p-Stat5a, rno_circRNA_007947-rno-miR-328a-3p-Stat5a, rno_circRNA_005064-rno-miR-18a-5p-Stat1, rno_circRNA_005064-rno-miR-18a-

5p-Stat5a, rno_circRNA_005115-rno-miR-22-3p-Stat1, rno_circRNA_009028-rno-miR-342-5p-Stat1, rno_circRNA_011240-rno-miR-1224-Stat5a, and rno_circRNA_016078-rno-miR-711-Stat5a.

Table 2. The top twenty up- or downregulated mRNAs in POF.

Gene name	log ₂ FC	FC	p-value	Control	POF
<i>HLA-DMB</i>	1.339337	2.53035	0.000703	3.960311	5.299648
<i>SCX</i>	1.251103	2.380233	0.027407	4.912758	6.163861
<i>FMO1</i>	1.181962	2.268852	0.034462	5.072154	6.254117
<i>TM7SF2</i>	1.159257	2.233424	0.007453	7.273177	8.432434
<i>AVP11</i>	1.062881	2.089099	0.021522	7.454662	8.517543
<i>CREG1</i>	1.010444	2.01453	0.006158	9.326441	10.33688
<i>PHLPB</i>	0.95061	1.93269	0.022663	5.07795	6.02856
<i>KLHDC8A</i>	0.914542	1.88497	0.01541	7.581941	8.496483
<i>RTP4</i>	0.883455	1.844788	0.044253	4.041173	4.924628
<i>KIF1A</i>	0.874577	1.833471	0.015266	5.560563	6.435141
<i>MVD</i>	0.859178	1.814005	0.020772	6.970943	7.830121
<i>RT1-BB</i>	0.849308	1.801637	0.04091	3.850027	4.699335
<i>TST</i>	0.830043	1.777739	0.026082	8.230059	9.060102
<i>SC4MOL</i>	0.829731	1.777354	0.011409	10.46872	11.29845
<i>RGD1306105</i>	0.824457	1.770869	0.02750	6.058627	6.883084
<i>RGD1563970</i>	0.822133	1.768018	0.04576	4.838298	5.660432
<i>AACS</i>	0.815731	1.76019	0.033827	6.79135	7.607082
<i>IRGM</i>	0.812023	1.755671	0.013265	4.466822	5.278845
<i>HMGCS1</i>	0.810962	1.754381	0.016833	9.649483	10.46044
<i>RAB31</i>	0.779148	1.716117	0.008018	6.337587	7.116735
<i>MGC72973</i>	-1.318907	0.400838	0.028898	10.4612	9.142297
<i>HBB</i>	-1.163998	0.446274	0.019027	10.96394	9.799939
<i>LOC689064</i>	-0.967847	0.511269	0.04029	10.66235	9.694503
<i>LOC501799</i>	-0.944384	0.519651	0.018445	8.031888	7.087504
<i>RGD1560207</i>	-0.915775	0.530059	0.014688	5.268186	4.352411
<i>B3GALT2</i>	-0.867188	0.548214	0.03276	5.537539	4.670351
<i>NPFFR1</i>	-0.862749	0.549904	0.00052	6.857978	5.995229
<i>LOC689244</i>	-0.858338	0.551588	0.028302	8.036131	7.177793
<i>RGD1564382</i>	-0.782047	0.581541	0.01782	5.137303	4.355256
<i>FAM122B</i>	-0.763428	0.589095	0.011551	6.507824	5.744397
<i>OMD</i>	-0.760595	0.590253	0.027355	9.168484	8.407889
<i>RGD1562220</i>	-0.740425	0.598563	0.003858	9.688917	8.948492
<i>LOC680073</i>	-0.738289	0.59945	0.004297	7.124413	6.386123
<i>LOC680643</i>	-0.730959	0.602503	0.002497	6.573561	5.842602
<i>SGOL2</i>	-0.725299	0.604872	0.044427	7.248221	6.522922
<i>LOC298442</i>	-0.703668	0.614009	0.006042	5.272925	4.569257
<i>CENPF</i>	-0.687667	0.620857	0.0298	7.27351	6.585843
<i>DBF4</i>	-0.680194	0.624081	0.024012	7.111396	6.431202
<i>CENPE</i>	-0.677426	0.62528	0.028993	6.313592	5.636167
<i>LOC690538</i>	-0.670059	0.628481	0.022419	7.574661	6.904602

FC, fold change.

3.5 Biological Implications of mRNAs Derived from the circRNA–miRNA–mRNA Network

Then, we investigated the biological implications of mRNAs derived from the circRNA–miRNA–mRNA network. Consequently, they exhibited prominent associations with biosynthetic (sterol, cholesterol, isoprenoid, steroid, lipid, *etc.*) and metabolic (cholesterol, sterol, alpha-amino acid, *etc.*) processes (Fig. 5A). Moreover, carboxylic acid binding, protein phosphatase binding, *etc.* (Fig. 5B) and

intracellular membrane-bounded organelles (Fig. 5C) were notably enriched. Various biosynthetic (steroid, terpenoid backbone, phenylalanine tyrosine, tryptophan, arginine, *etc.*) and metabolic (2-Oxocarboxylic acid, phenylalanine, cysteine, methionine, tyrosine, *etc.*) pathways were notably linked to mRNAs that formed the circRNA–miRNA–mRNA network (Fig. 5D). Specifically, we visualized the tyrosine metabolism pathway that was enriched by Aldh3b1 and Got1 (Fig. 5E).

3.6 Identification of POF-Specific Necroptosis Genes and any Underlying Molecular Mechanisms

Supplementary Fig. 1 illustrates the complex interactions between the differentially expressed mRNAs. Then, a PPI subnetwork of POF-specific-necroptosis genes was conducted, which comprised *STAT1*, *STAT5A*, *PLA2G4A*, *HMG1L1*, *HMGB1*, *AGER*, *EGFR*, *HDAC7*, *IFNA1*, *IL10RB*, *IL27RA*, *PYGL*, *SOCS1*, *TRADD*, *CXCL10*, *DDX5*, *EZH2*, *FADS2*, *FER*, *H2AFY2*, *HIST1H2AF*, *IFI44L*, *IL27*, *IRGM*, *MX1*, *NFKB2*, *PAFAH2*, *PEMT*, *PGM2L1*, *PGR*, *PHKA2*, and *PLB1* (Fig. 6A). Their differential expression was demonstrated in POF versus the controls (Fig. 6B). Afterward, the biological processes and KEGG pathways underlying POF-specific necroptosis genes were probed. Here, *H2AFY2*, *HMGB1*, *STAT1*, and *STAT5A* exhibited positive associations with the negative regulation of mitotic nuclear division and female meiotic nuclear division, while it also regulated the centrosome duplication processes and Fanconi anemia, homologous recombination, and the DNA replication pathways. Furthermore, negative correlations were found relating to the receptor signaling pathway, via JAK–STAT, in skeletal muscle fiber development, and cellular-modified amino acid catabolic processes alongside steroid biosynthesis, glycosaminoglycan degradation, and 2-Oxocarboxylic acid metabolism (Fig. 6C–J).

3.7 Landscape of POF Immunological Features

Utilizing the ssGSEA algorithm, we estimated the abundance of 28 immune cell types across POF and control specimens (Fig. 7A). Significant relationships between immune cells were observed (Fig. 7B). A higher abundance of most immune cells was exhibited in POF samples compared to the control, such as activated B cell, activated CD8⁺ T cell, activated dendritic cell, CD56 bright and CD56 dim natural killer cells, central memory CD4⁺ and CD8⁺ T cell, effector memory CD8⁺ T cell, macrophage, mast cell, T follicular helper cell, and Type 1 T helper cells (Fig. 7C). In addition, the current study observed differences between the POF and control samples in the transcriptional levels of immune checkpoints, chemokines, HLA molecules, and immune receptors (Fig. 7D–G).

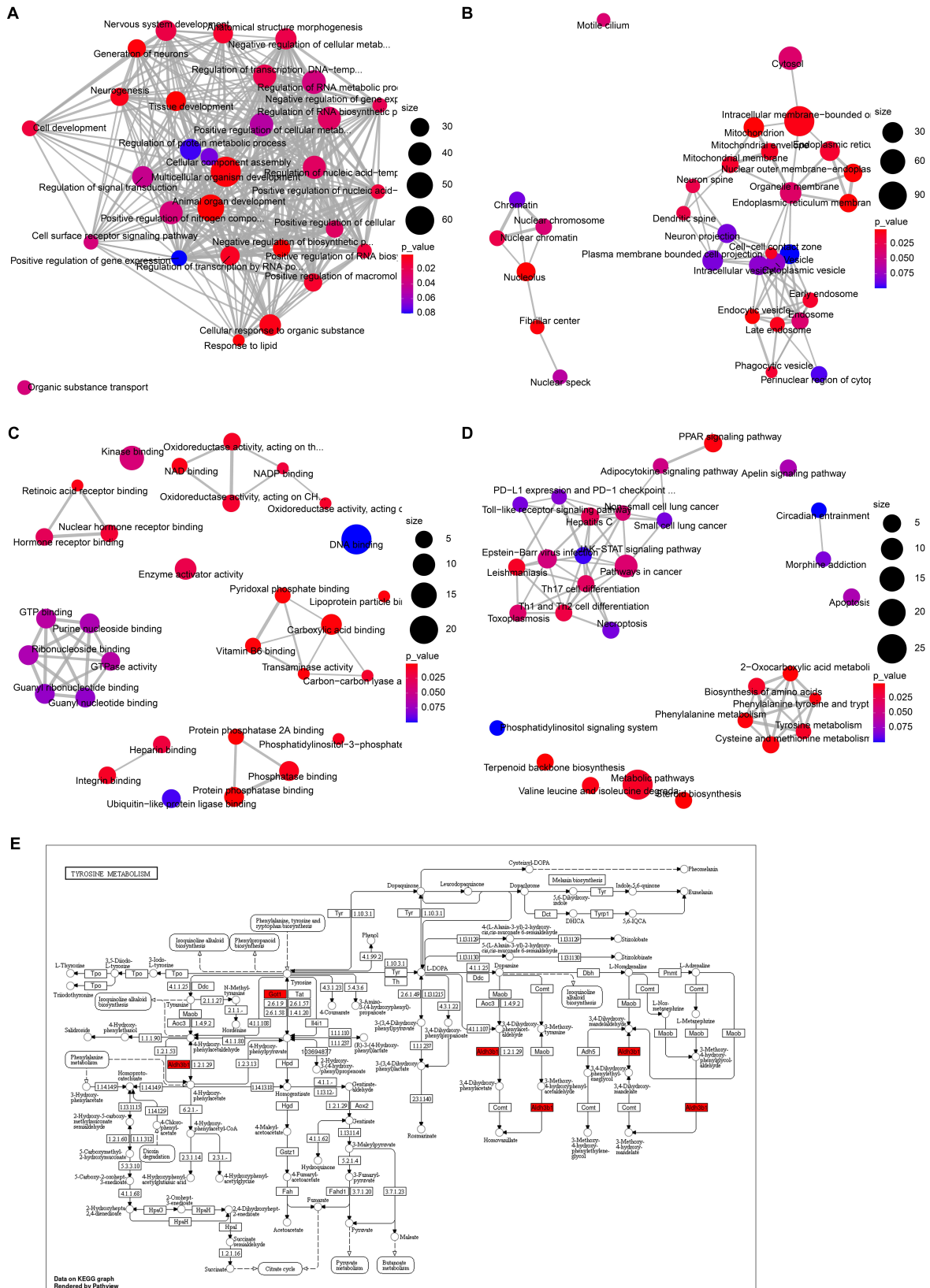


Fig. 5. Biological implications of mRNAs derived from the circRNA–miRNA–mRNA network. (A) Biological process, (B) molecular function, (C) cellular component, and (D) KEGG pathway terms for mRNAs derived from the circRNA–miRNA–mRNA network. (E) Visualization of the tyrosine metabolism pathway enriched by mRNAs derived from the circRNA–miRNA–mRNA network.

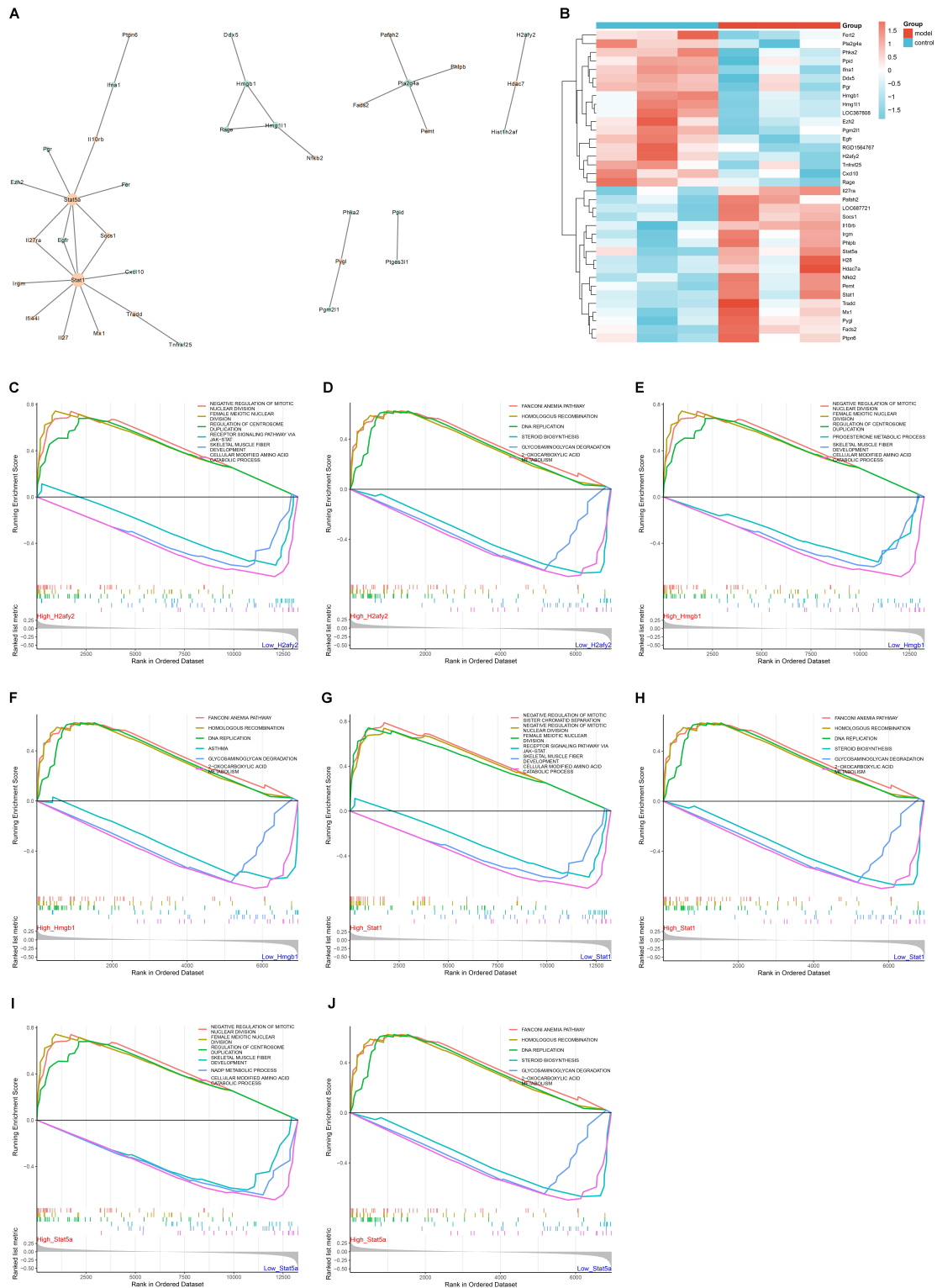


Fig. 6. Identification of POF-specific necroptosis genes and any underlying molecular mechanisms. (A) Protein–protein interaction (PPI) subnetwork depicts POF-specific necroptosis genes. (B) Heatmap exhibits the transcriptional levels of POF-specific necroptosis genes across POF and control specimens. Colors from blue to red indicate downregulated to upregulated levels of POF-specific necroptosis genes. (C,D) Gene set enrichment analysis (GSEA) unveils the biological processes and KEGG pathways significantly correlated to *H2AFY2*. (E,F) GSEA unveils the biological processes and KEGG pathways that exhibit significant correlations to *HMGB1*. (G,H) GSEA predicts the biological processes and KEGG pathways significantly associated with *STAT1*. (I,J) GSEA reveals the biological processes and KEGG pathways significantly linked to *STAT5A*.

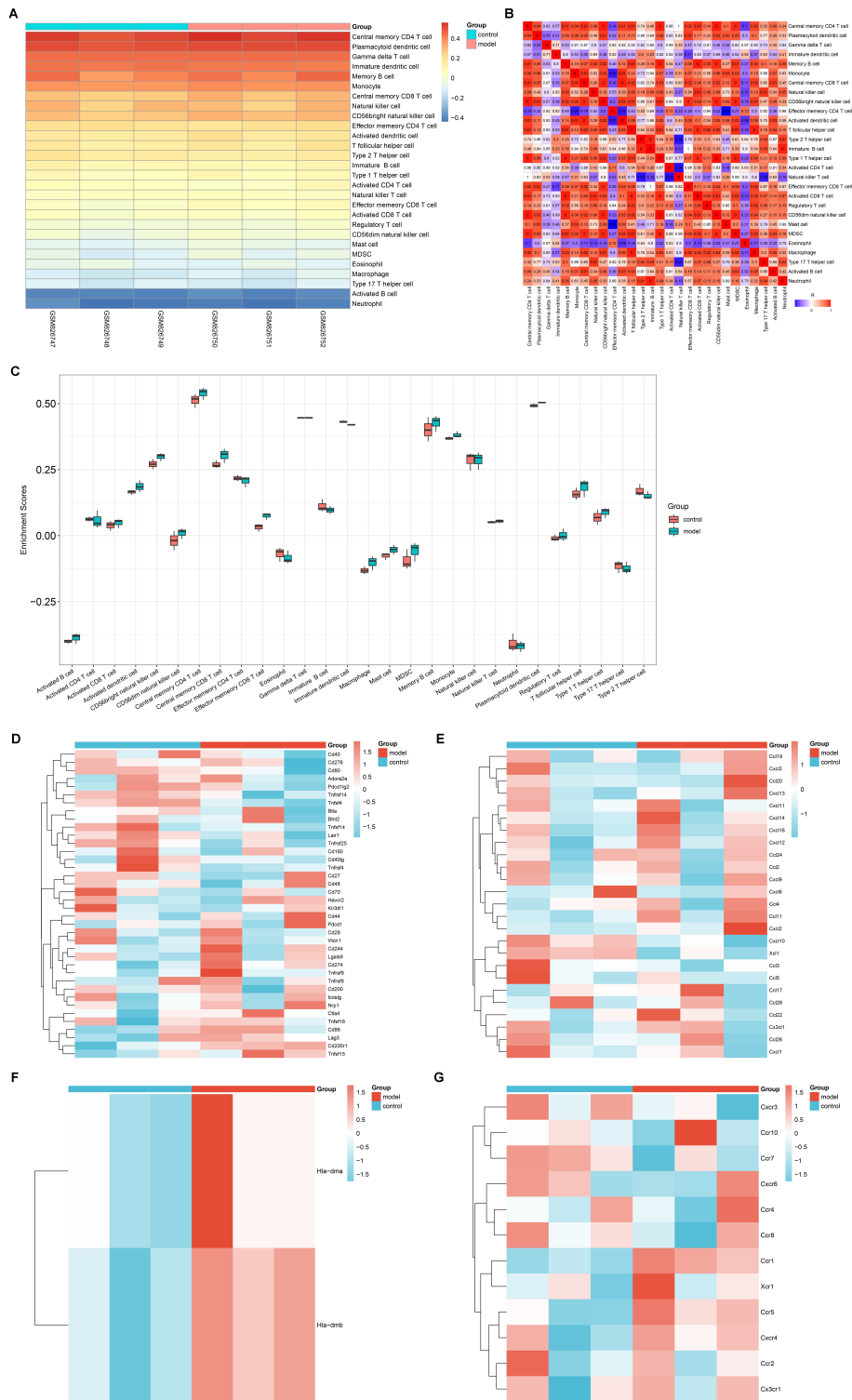


Fig. 7. Immunological features in POF. (A) Heatmap illustrates the abundance of diverse immune cell types across POF and control specimens. Colors from blue to red denote low to high infiltration of immune cells. (B) Heatmap exhibits the relationships between diverse immune cell types across POF and controls. Blue denotes the negative correlation coefficient, while red is the positive correlation coefficient. The shade of the colors is proportional to the correlation. *p*-value is marked in boxes. (C) Box plot illustrates the abundance score of diverse immune cell types in POF versus control specimens. (D) Heatmap visualizes the transcriptional levels of immune checkpoints across POF and controls. Colors from blue to red denote downregulated to upregulated transcriptional levels. (E–G) Heatmaps depict the transcriptional levels of (E) chemokines, (F) Human leukocyte antigen (HLA) molecules, and (G) immune receptors across POF and control specimens.

3.8 Associations of POF-Specific Necroptosis Genes with POF Immunological Features

Further analysis exhibited that POF-specific necroptosis genes were significantly linked to most immune cells (Fig. 8A), immune checkpoints (Fig. 8B), chemokines (Fig. 8C), HLA molecules (Fig. 8D), and immune receptors (Fig. 8E).

4. Discussion

POF pathogenesis is attributed to premature follicle loss owing to expedited atresia as well as mature or recruited primordial follicles that result in a folliculogenesis deficiency, which is an organized and complex process where small primordial follicles continue to mature into large ovulations anterior follicle [34]. Nonetheless, the molecular mechanisms underlying POF remain indistinct. CircRNAs are a form of single-stranded noncoding RNAs, which are circular in conformation owing to non-canonical splicing as well as back-splicing events [35]. Evidence has demonstrated that circRNAs participate in modulating granulosa cell functions [36]. For instance, Pan *et al.* [37] proposed that circRNA-induced inhibin-activin balance modulation in the apoptosis of ovarian granulosa cells as well as follicular atresia. Circular DDX10 exhibits an association with ovarian function via the modulation of proliferative capacity and steroidogenesis in granulosa cells [38]. Circ-ANKHD1 mediates granulosa cell apoptosis by targeting miR-27a-3p/SFRP1 signaling [39]. Circ-SLC41A1 is capable of resisting apoptosis in porcine granulosa cells and follicular atresia through miR-9820-5p/SRSF1 signaling [40]. These findings reveal that altered circRNAs participate in the onset of POF.

This study conducted circRNA sequencing analysis in ovarian tissues of POF and control rats to comprehensively analyze the expression profiles of circRNAs in POF. Previously, Chen *et al.* [41] performed circRNA microarray analysis of granulosa cells from females with POF and found that circRNAs with differential expression were predominantly linked to FoxO-related and cellular senescence pathways. In the current study, we identified abnormally expressed circRNAs and mRNAs in POF rats versus controls. Intriguingly, the differentially expressed mRNAs were found to be predominantly related to necroptosis. It has been accepted that DNA damage repair in ovarian granulosa cells exhibits a strong association with POF. Depleted oocytes with damaged DNA occur via distinct cellular death mechanisms, especially necroptosis [42]. However, limited evidence is available that proves the regulatory functions of circRNAs in cell death mechanisms. For instance, circRNA CNEACR attenuates necroptosis of cardiomyocytes in ischemia heart myocardial ischemia-reperfusion damage by suppressing Foxa2 expression [17]. In addition, circ_0004354 competes with circ_0040039 to trigger apoptosis and pyroptosis in nucleus pulposus cells as well as an inflammatory response by modulating miR-345-3p-FAF1/TP73 signaling in intervertebral disc

degeneration [43]. Herein, the current research established the circRNA-miRNA-mRNA networks of downregulated necroptosis genes (comprising rno_circRNA_004995-rno-miR-148b-5p-H2afy2, rno_circRNA_016998-rno-miR-29a-5p-Hmgb1, and rno_circRNA_017593-rno-miR-29a-5p-Hmgb1) and upregulated necroptosis genes (comprising rno_circRNA_015900-rno-miR-935-Stat1, rno_circRNA_007946-rno-miR-328a-3p-Stat5a, rno_circRNA_007947-rno-miR-328a-3p-Stat5a, rno_circRNA_005064-rno-miR-18a-5p-Stat1, rno_circRNA_005064-rno-miR-18a-5p-Stat5a, rno_circRNA_005115-rno-miR-22-3p-Stat1, rno_circRNA_009028-rno-miR-342-5p-Stat1, rno_circRNA_011240-rno-miR-1224-Stat5a, and rno_circRNA_016078-rno-miR-711-Stat5a). Our study indicated that these circRNAs might participate in the mediation of necroptosis in POF by serving as miRNA sponges and regulating the miRNA-targeted necroptosis mRNAs. Thus, these circRNAs might become potential diagnostic and therapeutic targets for POF.

Based upon the PPI subnetwork, we determined POF-specific necroptosis genes (*STAT1*, *STAT5A*, *PLA2G4A*, *HMG1L1*, *HMGB1*, *AGER*, *EGFR*, *HDAC7*, *IFNA1*, *IL10RB*, *IL27RA*, *PYGL*, *SOCS1*, *TRADD*, *CXCL10*, *DDX5*, *EZH2*, *FADS2*, *FER*, *H2AFY2*, *HIST1H2AF*, *IFI44L*, *IL27*, *IRGM*, *MX1*, *NFKB2*, *PAFAH2*, *PEMT*, *PGM2L1*, *PGR*, *PHKA2*, AND *PLB1*), which exhibited abnormal expressions in POF samples compared to the controls, thereby further proving the aberrantly regulated necroptosis process in POF. Accumulated evidence unveils immune dysfunction in POF. For instance, the up-regulation of circulating CD8⁺ CD28⁻ T cells can restore ovarian functions in POF mice [44]. In addition, attenuating the ratios of T-helper 17 (Th17)/cytotoxic T and Th17/Treg cells improved ovarian functions in POF mice [45]. During necroptosis, the dying cells are ruptured and release intracellular components, thereby triggering an innate immune response [46]. The current study displayed the notable associations of POF-specific necroptosis genes with most immune cells, immune checkpoints, chemokines, HLA molecules, and immune receptors, thereby proving the presence of relationships between necroptosis and immunity and immune responses in POF.

However, the limitations of our study should be highlighted. Although we identified the circRNA-mediated post-transcriptional regulatory mechanisms underlying necroptosis in POF, further experimental validation is required. Thus, in future studies, we will further validate our findings on the regulatory mechanisms of circRNAs in necroptosis. Furthermore, we found that necroptosis genes were remarkably linked to immunity and immune responses in POF. Therefore, our future research will conduct an in-depth analysis of the interactions between necroptosis and immunity and immune responses as well as their interactions in POF.

5. Conclusions

In summary, the present research proposed the widespread regulatory mechanisms of circRNAs in necroptosis during POF, demonstrating that abnormal circRNA biogenesis can potentially affect necroptosis, which might result in the onset of POF.

Abbreviations

POF, premature ovarian failure; circRNAs, circular RNAs; miRNAs, microRNAs; FC, fold change; ceRNA, competitive endogenous RNA; PPI, protein-protein interaction; KEGG, Kyoto Encyclopedia of Genes and Genomes; GSEA, gene set enrichment analysis; FDR, false discovery rate; ssGSEA, single-cell GSEA; HLA, human leukocyte antigen.

Availability of Data and Materials

The data used to support the findings of this study are included within the supplementary information files.

Author Contributions

WC conceived and designed the study. XJ, JW and XX conducted most of the experiments and data analysis, and wrote the manuscript. TZ, LW and XF participated in collecting data and helped to draft the manuscript. All authors reviewed and approved the final manuscript. All authors have participated sufficiently in the work and agreed to be accountable for all aspects of the work.

Ethics Approval and Consent to Participate

This project gained the approval of the Animal Ethical and Welfare Committee of Zhejiang Chinese Medical University (IACUC-20210503-05).

Acknowledgment

Not applicable.

Funding

This work was funded by The National Natural Science Foundation of China (Grant No. 82004405), The Exploration Project of Natural Science Foundation of Zhejiang Province (Grant No. LQ20H270005) and Zhejiang Province Traditional Chinese Medicine Science and technology Project (Grant No. 2023ZL366).

Conflict of Interest

The authors declare no conflict of interest.

Supplementary Material

Supplementary material associated with this article can be found, in the online version, at <https://doi.org/10.31083/j.fbl2811314>.

References

- [1] Qu Q, Liu L, Cui Y, Liu H, Yi J, Bing W, *et al.* miR-126-3p containing exosomes derived from human umbilical cord mesenchymal stem cells promote angiogenesis and attenuate ovarian granulosa cell apoptosis in a preclinical rat model of premature ovarian failure. *Stem Cell Research & Therapy.* 2022; 13: 352.
- [2] Wang L, Mei Q, Xie Q, Li H, Su P, Zhang L, *et al.* A comparative study of Mesenchymal Stem Cells transplantation approach to antagonize age-associated ovarian hypofunction with consideration of safety and efficiency. *Journal of Advanced Research.* 2021; 38: 245–259.
- [3] Blümel JE, Mezones-Holguín E, Chedraui P, Soto-Becerra P, Arteaga E, Vallejo MS. Is premature ovarian insufficiency associated with mortality? A three-decade follow-up cohort. *Maturitas.* 2022; 163: 82–87.
- [4] Du D, Tang X, Li Y, Gao Y, Chen R, Chen Q, *et al.* Senotherapy Protects against Cisplatin-Induced Ovarian Injury by Removing Senescent Cells and Alleviating DNA Damage. *Oxidative Medicine and Cellular Longevity.* 2022; 2022: 9144644.
- [5] Mittal M, McEniery C, Supramaniam PR, Cardozo L, Savvas M, Panay N, *et al.* Impact of micronised progesterone and medroxyprogesterone acetate in combination with transdermal oestradiol on cardiovascular markers in women diagnosed with premature ovarian insufficiency or an early menopause: a randomised pilot trial. *Maturitas.* 2022; 161: 18–26.
- [6] Misir S, Wu N, Yang BB. Specific expression and functions of circular RNAs. *Cell Death and Differentiation.* 2022; 29: 481–491.
- [7] Liu CX, Chen LL. Circular RNAs: Characterization, cellular roles, and applications. *Cell.* 2022; 185: 2016–2034.
- [8] Chen L, Huang C, Shan G. Circular RNAs in physiology and non-immunological diseases. *Trends in Biochemical Sciences.* 2022; 47: 250–264.
- [9] Chen L, Wang C, Sun H, Wang J, Liang Y, Wang Y, *et al.* The bioinformatics toolbox for circRNA discovery and analysis. *Briefings in Bioinformatics.* 2021; 22: 1706–1728.
- [10] Liu C, Zhu X, Niu X, Chen L, Ge C. Elevated hsa_circRNA_101015, hsa_circRNA_101211, and hsa_circRNA_103470 in the Human Blood: Novel Biomarkers to Early Diagnose Acute Pancreatitis. *BioMed Research International.* 2020; 2020: 2419163.
- [11] He AT, Liu J, Li F, Yang BB. Targeting circular RNAs as a therapeutic approach: current strategies and challenges. *Signal Transduction and Targeted Therapy.* 2021; 6: 185.
- [12] Gao Y, Shang S, Guo S, Li X, Zhou H, Liu H, *et al.* Lnc2Cancer 3.0: an updated resource for experimentally supported lncRNA/circRNA cancer associations and web tools based on RNA-seq and scRNA-seq data. *Nucleic Acids Research.* 2021; 49: D1251–D1258.
- [13] Weindel CG, Martinez EL, Zhao X, Mabry CJ, Bell SL, Vail KJ, *et al.* Mitochondrial ROS promotes susceptibility to infection via gasdermin D-mediated necroptosis. *Cell.* 2022; 185: 3214–3231.e23.
- [14] Niu X, Chen L, Li Y, Hu Z, He F. Ferroptosis, necroptosis, and pyroptosis in the tumor microenvironment: Perspectives for immunotherapy of SCLC. *Seminars in Cancer Biology.* 2022; 86: 273–285.
- [15] Zhang T, Yin C, Fedorov A, Qiao L, Bao H, Beknazarov N, *et al.* ADAR1 masks the cancer immunotherapeutic promise of ZBP1-driven necroptosis. *Nature.* 2022; 606: 594–602.
- [16] Li H, Jing Y, Qu X, Yang J, Pan P, Liu X, *et al.* The Activation of Reticulophagy by ER Stress through the ATF4-MAP1LC3A-CCPG1 Pathway in Ovarian Granulosa Cells Is Linked to Apoptosis and Necroptosis. *International Journal of Molecular Sciences.* 2023; 24: 2749.

- [17] Gao XQ, Liu CY, Zhang YH, Wang YH, Zhou LY, Li XM, *et al.* The circRNA CNEACR regulates necroptosis of cardiomyocytes through Foxa2 suppression. *Cell Death and Differentiation*. 2022; 29: 527–539.
- [18] Ritchie ME, Phipson B, Wu D, Hu Y, Law CW, Shi W, *et al.* limma powers differential expression analyses for RNA-seq and microarray studies. *Nucleic Acids Research*. 2015; 43: e47.
- [19] Nilsson E, Larsen G, Manikkam M, Guerrero-Bosagna C, Savenkova MI, Skinner MK. Environmentally induced epigenetic transgenerational inheritance of ovarian disease. *PLoS ONE*. 2012; 7: e36129.
- [20] Wu W, Ji P, Zhao F. CircAtlas: an integrated resource of one million highly accurate circular RNAs from 1070 vertebrate transcriptomes. *Genome Biology*. 2020; 21: 101.
- [21] Agarwal V, Bell GW, Nam JW, Bartel DP. Predicting effective microRNA target sites in mammalian mRNAs. *eLife*. 2015; 4: e05005.
- [22] Wong N, Wang X. miRDB: an online resource for microRNA target prediction and functional annotations. *Nucleic Acids Research*. 2015; 43: D146–D152.
- [23] Huang HY, Lin YCD, Li J, Huang KY, Shrestha S, Hong HC, *et al.* miRTarBase 2020: updates to the experimentally validated microRNA-target interaction database. *Nucleic Acids Research*. 2020; 48: D148–D154.
- [24] Shannon P, Markiel A, Ozier O, Baliga NS, Wang JT, Ramage D, *et al.* Cytoscape: a software environment for integrated models of biomolecular interaction networks. *Genome Research*. 2003; 13: 2498–2504.
- [25] von Mering C, Huynen M, Jaeggi D, Schmidt S, Bork P, Snel B. STRING: a database of predicted functional associations between proteins. *Nucleic Acids Research*. 2003; 31: 258–261.
- [26] Ashburner M, Ball CA, Blake JA, Botstein D, Butler H, Cherry JM, *et al.* Gene ontology: tool for the unification of biology. The Gene Ontology Consortium. *Nature Genetics*. 2000; 25: 25–29.
- [27] Kanehisa M, Goto S. KEGG: kyoto encyclopedia of genes and genomes. *Nucleic Acids Research*. 2000; 28: 27–30.
- [28] Luo W, Pant G, Bhavnasi YK, Blanchard SG, Jr, Brouwer C. Pathview Web: user friendly pathway visualization and data integration. *Nucleic Acids Research*. 2017; 45: W501–W508.
- [29] Subramanian A, Tamayo P, Mootha VK, Mukherjee S, Ebert BL, Gillette MA, *et al.* Gene set enrichment analysis: a knowledge-based approach for interpreting genome-wide expression profiles. *Proceedings of the National Academy of Sciences of the United States of America*. 2005; 102: 15545–15550.
- [30] Hänzelmann S, Castelo R, Guinney J. GSEA: gene set variation analysis for microarray and RNA-seq data. *BMC Bioinformatics*. 2013; 14: 7.
- [31] Charoentong P, Finotello F, Angelova M, Mayer C, Efremova M, Rieder D, *et al.* Pan-cancer Immunogenomic Analyses Reveal Genotype-Immunophenotype Relationships and Predictors of Response to Checkpoint Blockade. *Cell Reports*. 2017; 18: 248–262.
- [32] Bindea G, Mlecnik B, Tosolini M, Kirilovsky A, Waldner M, Obenauf AC, *et al.* Spatiotemporal dynamics of intratumoral immune cells reveal the immune landscape in human cancer. *Immunity*. 2013; 39: 782–795.
- [33] Zheng XL, Yang JJ, Wang YY, Li Q, Song YP, Su M, *et al.* RIP1 promotes proliferation through G2/M checkpoint progression and mediates cisplatin-induced apoptosis and necroptosis in human ovarian cancer cells. *Acta Pharmacologica Sinica*. 2020; 41: 1223–1233.
- [34] Qin X, Zhao Y, Zhang T, Yin C, Qiao J, Guo W, *et al.* TrkB agonist antibody ameliorates fertility deficits in aged and cyclophosphamide-induced premature ovarian failure model mice. *Nature Communications*. 2022; 13: 914.
- [35] Marfil-Marin E, Santamaria-Olmedo M, PerezGrovas-Saltijeral A, Valdes-Flores M, Ochoa-Morales A, Jara-Prado A, *et al.* circRNA Regulates Dopaminergic Synapse, MAPK, and Long-term Depression Pathways in Huntington Disease. *Molecular Neurobiology*. 2021; 58: 6222–6231.
- [36] Zhou J, Zhou J, Wu LJX, Li YY, Li MQ, Liao HQ. CircRNA circUSP36 impairs the stability of NEDD4L mRNA through recruiting PTBP1 to enhance ULK1-mediated autophagic granulosa cell death. *Journal of Reproductive Immunology*. 2022; 153: 103681.
- [37] Ma M, Wang H, Zhang Y, Zhang J, Liu J, Pan Z. circRNA-Mediated Inhibin-Activin Balance Regulation in Ovarian Granulosa Cell Apoptosis and Follicular Atresia. *International Journal of Molecular Sciences*. 2021; 22: 9113.
- [38] Cai H, Chang T, Li Y, Jia Y, Li H, Zhang M, *et al.* Circular *DDX10* is associated with ovarian function and assisted reproductive technology outcomes through modulating the proliferation and steroidogenesis of granulosa cells. *Aging*. 2021; 13: 9592–9612.
- [39] Li X, Gao F, Fan Y, Xie S, Li C, Meng L, *et al.* A novel identified circ-ANKHD1 targets the miR-27a-3p/SFRP1 signaling pathway and modulates the apoptosis of granulosa cells. *Environmental Science and Pollution Research International*. 2021; 28: 57459–57469.
- [40] Wang H, Zhang Y, Zhang J, Du X, Li Q, Pan Z. circSLC41A1 Resists Porcine Granulosa Cell Apoptosis and Follicular Atresia by Promoting SRSF1 through miR-9820-5p Sponging. *International Journal of Molecular Sciences*. 2022; 23: 1509.
- [41] Zhou XY, Li Y, Zhang J, Liu YD, Zhe J, Zhang QY, *et al.* Expression profiles of circular RNA in granulosa cells from women with biochemical premature ovarian insufficiency. *Epigenomics*. 2020; 12: 319–332.
- [42] Sha C, Chen L, Lin L, Li T, Wei H, Yang M, *et al.* TRDMT1 participates in the DNA damage repair of granulosa cells in premature ovarian failure. *Aging*. 2021; 13: 15193–15213.
- [43] Li Y, Wu X, Li J, Du L, Wang X, Cao J, *et al.* Circ_0004354 might compete with circ_0040039 to induce NPCs death and inflammatory response by targeting miR-345-3p-FAF1/TP73 axis in intervertebral disc degeneration. *Oxidative Medicine and Cellular Longevity*. 2022; 2022: 2776440.
- [44] Yin N, Wu C, Qiu J, Zhang Y, Bo L, Xu Y, *et al.* Protective properties of heme oxygenase-1 expressed in umbilical cord mesenchymal stem cells help restore the ovarian function of premature ovarian failure mice through activating the JNK/Bcl-2 signal pathway-regulated autophagy and upregulating the circulating of CD8⁺CD28⁻ T cells. *Stem Cell Research & Therapy*. 2020; 11: 49.
- [45] Yin N, Wang Y, Lu X, Liu R, Zhang L, Zhao W, *et al.* hPMSC transplantation restoring ovarian function in premature ovarian failure mice is associated with change of Th17/Tc17 and Th17/Treg cell ratios through the PI3K/Akt signal pathway. *Stem Cell Research & Therapy*. 2018; 9: 37.
- [46] Newton K, Manning G. Necroptosis and Inflammation. *Annual Review of Biochemistry*. 2016; 85: 743–763.